ZnO photonic crystal lasers

Xiaohua Wu[a], Alexey Yamilov[a,b], Xiang Liu[c], Shuyou Li[c], Vinayak P. Dravid[c], Robert P. H. Chang[c], Hui Cao[a]

[a]Dept. of Phys. and Astro., Northwestern Univ. 2145 Sheridan Rd, Evanston, IL, 60208
[b]Dept. of Phys., Univ. of Missouri-Rolla, 1870 Miner Circle, Rolla, MO, 65409
[c]Dept. of Mate. Sci. and Engi. Northwestern Univ. 2145 Sheridan Rd, Evanston, IL, 60208

ABSTRACT

We fabricated two dimensional photonic crystal structures in zinc oxide films with focused ion beam etching. Lasing is realized in the near ultraviolet frequency at room temperature under optical pumping. From the measurement of lasing frequency and spatial profile of the lasing modes, as well as the photonic band structure calculation, we conclude that lasing occurs in either localized or extended defect modes near the dielectric edge of photonic band gap. These defect modes originate from the structure disorder unintentionally introduced during the fabrication process. Fine tuning of lasing wavelength across 20nm range has been realized by varying the lattice constant of PhCS structure. A qualitative explanation for these PhCS lasers with self optimization of laser cavity quality factor has been proposed.

Keywords: ZnO, defect mode, PhCS, laser, self optimization

1. INTRODUCTION

A photonic crystal slab (PhCS) is a dielectric layer with in-plane two-dimensional (2D) photonic crystals structures. Such device has attracted much attention because of their potential applications to various optoelectronic devices and circuits.[1] Defect cavities in these photonic devices can have high quality factor and small modal volume.[2–6] The in-plane light confinement is achieved for frequency within photonic band gap formed by Bragg interference, while the index guiding prevents light leakage in the perpendicular direction. So far many Low-threshold lasing has been realized in PhCS made of III-V semiconductors.[7–10] They operate in the near infrared or infrared communication frequencies. PhCS lasers with emission at ultra-violet (UV) region are much more challenging because: first, the smaller feature size for a in plane UV stop band, second, the difficulty in wide band gap materials (e.g., GaN, ZnO) etching. On the other hand, the demand for blue and UV compact light sources has prompted enormous research effort into wide band gap semiconductors.[11] Recently we reported the first realization of UV photonic crystal laser that operates at room temperature.[12] Compared with other wide band gap materials, ZnO has the advantage of large exciton binding energy ($\sim$ 60 meV), that allows efficient excitonic emission even at room temperature.

The commonly fabricated PhCS of III-V semiconductors are mostly a bridged membrane structure, whose substrate is selectively etched away so both above and under the photonic layer are air. Though such structure can achieve wider in plane photonic band gap and better light confinement in the vertical direction, it is usually mechanically fragile and poorly heat dissipated. Also it is difficult to make a large area fabrication and can not be applied to on chip fabrication easily. In our case, ZnO photonic layer is fabricated on lattice matched sapphire substrate. Such structure is much more solid and easier for on chip applications with large scales. On the other hand, due to the less refractive index contrast between the photonic layer and substrate, the light confinement in the vertical direction is worse than that in III-V semiconductors, and the in plane photonic band gap is also narrower. In this case, the defects introduced during fabrication are supposed to be more detrimental to PhCS lasers. However, we still successfully achieved lasing in such ZnO PhCS at room temperature. A self-optimization theory is given to qualitatively explain this experimental phenomenon.

Further author information: h-cao@northwestern.edu, Tel: 1 847-467-5452 Fax: 847-491-9982

Zinc Oxide Materials and Devices, edited by Ferechteh Hosseini Teherani, Cole W. Litton,
Proc. of SPIE Vol. 6122, 612205, (2006) · 0277-786X/06/$15 · doi: 10.1117/12.645454

The structure of this paper is as following: in section I, we design a ZnO PhCS structure with in plane photonic band using a plane wave expansion method, and the structure parameters for maximum gap width are presented at the end. In section II, we describe the experimental details for sample fabrication and optical measurement, and experimental results for lasing are presented as well. In section III, we discuss the experimental data with a qualitatively explanation of self optimization process in our PhCS laser, and finally make a conclusion.

2. THEORY

To design the optimum PhCS structure in our ZnO film on sapphire substrate, a simulation has been done with a plane-wave expansion method.[13] Our ZnO PhCS is vertically asymmetric: with air on top and sapphire substrate at bottom. To apply the plane-wave expansion method for photonic band calculation, we considered a super unit cell that consists of air, ZnO photonic crystal slab, sapphire substrate, ZnO photonic crystal slab and air (see the inset of Fig. 1). Detailed simulation results can be found in another reference.[15] The guided modes confined to the PhCS should lie inside the ZnO/substrate light cone and the air/ZnO light cone. Due to a particular arrangement of the layers in our supercell, there exists an artificial reflection symmetry with plane Σ_{sc}. Therefore, there is an artificial classification of the modes into symmetric and antisymmetric, as it is schematically shown in inset of Fig. 1. This property provides a way to control the precision of the band structure calculation. Indeed, only for the PhCS-guided modes (with eigenfrequencies outside of the air and substrate light cone), and only when the substrate is thick enough, the guided modes in the two ZnO layers are decoupled, and the symmetric and antisymmetric modes should be degenerate in eigenfrequency. This artificial degeneracy is used as the check of consistency in our band structure calculations.

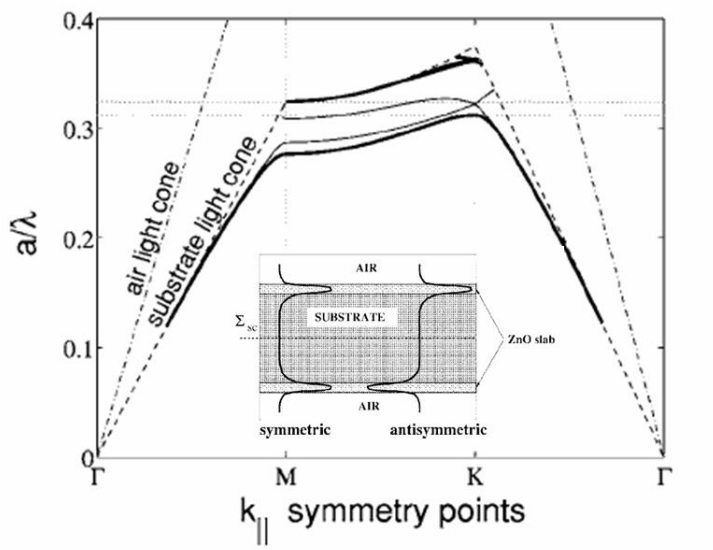

Figure 1. Calculated band structure of ZnO PhCS, air cylinder radius $r/a = 0.25$, and slab thickness $t/a = 1.4$. The refractive indexes for ZnO and sapphire are 2.35 and 1.78. Thin and thick lines represent TM and TE polarized modes respectively. Inset are the super cell of our simulation, the reflection symmetry allows for solutions symmetric and antisymmetric with regard to reflection in Σ_{sc}.

In Fig. 1 we show an example of the calculated photonic band structure. Air light-cone boundary, $\omega = ck_{//}$, and substrate light-cone boundary, $\omega = (c/n_s)k_{//}$ are shown with dashdot and dashed lines, respectively. The

presence of a sapphire cone makes guiding at the Γ point impossible and limits any band gap to $a/\lambda < 0.325$. For PhCS laser operation we need to overlap a photonic band gap with a gain spectrum of ZnO, $380nm < \lambda < 400nm$. Consequently, the lattice constant in the hexagonal air-hole pattern of PhCS has an upper bound of $a < 130nm$. In a symmetric PhCS (i.e. the substrate is replaced by air), the modes can be grouped into two classes: modes that have z-component of the magnetic field or electric field symmetric with respect to the center plane of the photonic layer. Low lying modes of the first/second class are mainly transverse electric/magnetic (TE/TM) polarized. This separability was crucial for obtaining a sizable PBG in a photonic membrane and complete stop bands for the guided modes of each class can exist independently.[16] The presence of the sapphire substrate in our ZnO PhCS removes the symmetry,[17] and there are mixes up of polarizations for its eigenmodes. we calculated the field components of the first five bands with and without the sapphire substrate and found close resemblance in the spatial profiles of the corresponding modes in the two cases. This is due to strong vertical confinement of the guided modes. Therefore, the modes in the ZnO PhCS with the sapphire substrate can still be classified as predominantly either TE-like or TM-like. Careful calculation of all the electric and magnetic field components shows that the first and fourth modes are TE-like dominant, while the second and third modes are TM-like dominant for the band structures shown in Fig 1. So there is a photonic band gap for TE-like guided modes in this ZnO PhCS as shown between the two dotted lines. The abandon of TM-like modes are justified by the experimental facts that the polarization of ZnO exciton emission is mostly perpendicular to the c-axis.[18, 19] Since the c-axis of our ZnO film is normal to the film/substrate interface, the emitted photons are coupled mainly into TE-like modes, as we confirmed experimentally from the measurement of polarization of photoluminescence from the side of an unpatterned ZnO film.

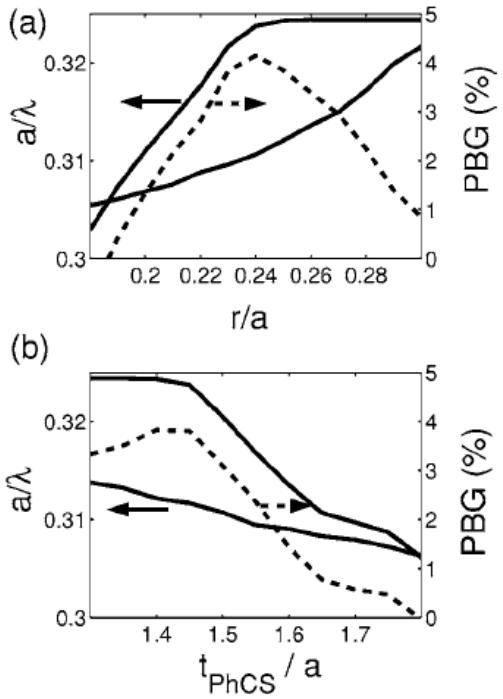

Figure 2. The position and relative size of photonic band gap for PhCS with variable structure parameters. (a) $t_{ph}/a = 1.4$; (b) $r/a = 0.25$. Refractive index 2.35 and 1.78 are used for ZnO and sapphire in this calculation. The left vertical axes should be used with solid lines, which represent the edges of PBG. Dashed lines and right vertical axes show the relative size of the gap.

We intend to optimize the relative width (normalized to the center frequency) of photonic band gap in our ZnO PhCS structure by varying two parameters independently: (i) air hole radius r, (ii) photonic layer thickness

t_{ph}. Due to linear nature of Maxwell equations, we normalize all parameters to the value of lattice constant, a. From the experimental prospective it is difficult to reproduce extremely small structural features, therefore we prefer to have PBG at high values of a/λ if possible. Fig. 2 shows the results of our simulation. In panel (a) we plot the position and relative width of the PhCS as we vary r/a within the range of 0.18-0.30, and keep $t_{ph}/a = 1.4$. One can clearly see that there exists a PBG maximum at $r/a \approx 0,24$. This effect has a clear physical interpretation: at large filling fractions (small r/a) the index contrast within the PhCS is small, therefore band splitting, as well as PBG, is small. At small filling fractions, the waveguiding becomes poor, furthermore the decrease of the effective refractive index of the photonic layer leads to a shift of the PBG as a whole to higher frequency. In panel (b) we plot the position and relative width of the PhCS as we vary t_{ph}/a from 1.3 to 1.8, while keeping $r/a = 0.25$. It can be seen that the gap can be maximized at $t_{ph}/a \approx 1.45$. this can also be understood physically: at small t_{ph}/a, the photonic layer is so thin that the waveguiding is poor, and at large t_{ph}/a, the number of guided modes increase too much to permit a photonic gap in this PhCS. In conclusion, the maximum gap width 0.04 can be achieved at $t_{ph}/a \approx 1.45$ and $r/a \approx 0,24$, and the center frequency is at $a/\lambda \approx 0.315$. Applying these parameters to our ZnO PhCS experimental realization and taking $\lambda = 390nm$, we get $a = 123nm$, $r = 30nm$ and $t_{ph} = 178nm$ for maximum photonic gap width.

3. EXPERIMENT

Experimentally the 2D triangular lattice photonic crystal structure is fabricated in ZnO films. First, 200 nm thick ZnO films are grown on c-plane sapphire substrates by plasma enhanced MOCVD at 750^o C. The selected area electron diffraction pattern of the film reveals that single crystalline ZnO is grown along the c-axis. Next, triangular latticed arrays of cylindrical air columns are etched in the films by focused Ga^{3+} ion beam accelerated at 30 KeV and 30 pA current. FIB has been widely used for maskless and resistless nano-scale patterning, it allows us to precisely control the position, size and density of air cylinders in the ZnO films. Due to the small hole size ($r \approx 30nm$) and the limitation of etching facilities, some deviation from perfect periodic structures are unavoidable. It can be seen in the SEM image of one of our typical PhCS sample shown in Fig. 3. The air holes are not perfectly circular due to the facility resolution limit and drifting of sample during etching process. The side wall of air holes is very close to vertical with a little smaller radius at bottom, which is not shown here. The etched patterns are usually $8\mu m \times 8\mu m$, and the photonic layer is a little thinner than the film at unpatterned area due to the etching. The ZnO crystalline quality are seriously damaged by the bombardment of Ga ions during the FIB etching procedure, and the photoluminescence emission from the patterned area is much quenched compared to unpatterned area. To remove such damage, we annealed the patterned films in O_2 at 600^oC for one hour and found that the emission are partially recovered. To test the photonic band gap effect, we first fabricated PhCS patterns with different lattice constant a from 100nm to 160nm with a large step size of 15nm. The air hole radius r is scaled with a at a fix ratio of 0.25. From our simulation, we would expect that the patterns with $a = 115nm$ and 130nm would lase at lower threshold comparing to others due to the photonic gap effect.

The samples are optically pumped by the third harmonics of a mode-locked Nd:YAG laser (355 nm, 10 Hz, 20 ps) at room temperature. We used the picosecond pump laser simply because of its availability. Since the pump pulse is much shorter than the lifetime of exciton in ZnO, the peak power required to reach the lasing threshold would be much higher than that with nanosecond pump pulses. A 10× microscope objective lens (N.A.=0.25) is used to focus the pump beam, and the pump spot size can be varied by changing the distance between the pump lens and sample surface. In a typical experiment, a $6\mu m$ diameter pumping spot is used. Since the sapphire substrate is double-side polished and transparent in both visible and UV frequencies, a 20× microscope objective lens (N.A.=0.40) is placed at the back side of the sample for both collection of emitted light and simultaneous measurement of the spatial distribution of lasing mode. Then the emitted light is coupled into a UV fiber, which is connected to a spectrometer with 0.13 nm spectral resolution. The pump light is blocked by a bandpass filter, while the image of lasing mode profile is projected by the objective lens onto a UV sensitive CCD camera. The sample is also illuminated by a white light source so that we can identify the position of the lasing modes in the photonic lattice.

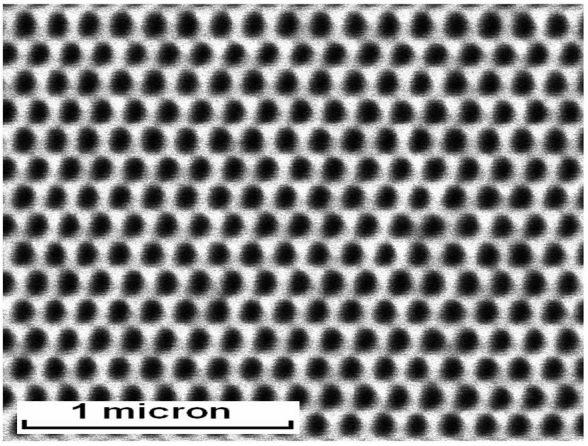

Figure 3. A top-view SEM of one ZnO PhCS sample. The lattice constant $a = 125nm$ and air cylinder radius $r/a = 0.25$.

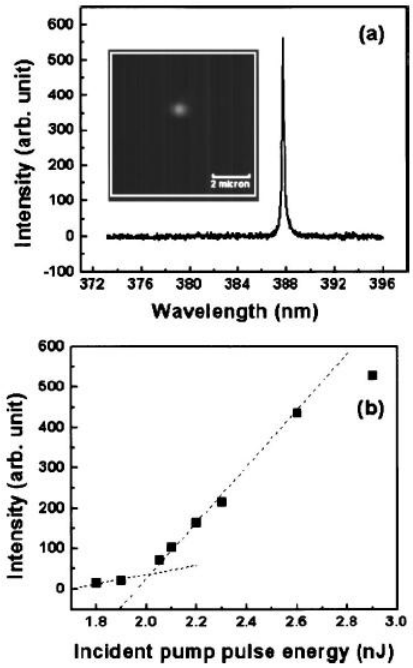

Figure 4. (a) Lasing spectrum of a ZnO PhCS with $a = 115nm$ shows a single defect mode. The pump pulse energy is 2.3nJ. Inset is the near field image of the lasing mode. (b) Emission intensity of the defect mode vs the incident pump pulse energy.

Among all fabricated patterns with lattice constant a varying from 100nm to 160 nm, lasing is realized only in the structures of $a = 115nm$ and $a = 130nm$. Fig. 4(a) shows the spectrum of emission from a pattern of a =115 nm and $r/a = 0.25$. It has a single sharp peak at 387.7 nm. Fig. 4(b) plots the emission intensity integrated over this peak as a function of the incident pump pulse energy. Note that not all the pump light incident onto the sample is absorbed, part of it is transmitted, reflected or scattered. It is difficult to measure the exact percentage of the incident pump being absorbed. Nevertheless, the threshold behavior is clearly seen in Fig. 4(b). Above the threshold, the spectral width of this lasing peak is only 0.24 nm. These data indicate that lasing oscillation occurs in this structure. The near-field image of this lasing mode is obtained simultaneously

and shown in the inset of Fig. 4(a). The white square marks the boundary of the triangular lattice. The lasing mode is spatially localized in a small region of $\sim$1.0 μm^2 inside the lattice. As we move the pump spot across the lattice, the lasing modes change in both frequency and spatial pattern. This behavior suggests that this lasing mode is spatially localized defect state. It is formed by the short range structural disorder[14] which are introduced unintentionally during fabrication. Lasing is also observed at longer wavelength for the pattern with a=130 nm and $r/a = 0.25$ with higher lasing threshold.

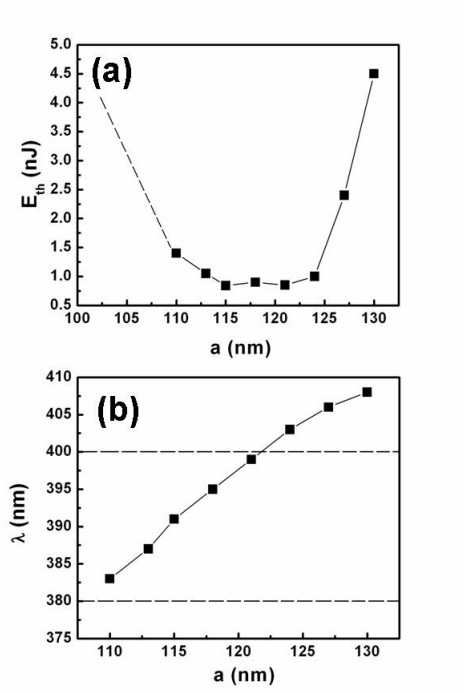

Figure 5. (a) Experimentally measured incident pump pulse energy at the lasing threshold as a function of lattice constant a. Dash line indicates that samples with $a < 110nm$ don't lase at shown pump pulse energy range. (b) Measured lasing mode wavelength as a function of lattice constant a. Dash lines at $\lambda = 380nm$ and 400nm are edges of gain spectrum of ZnO.

To carefully study the lasing modes from ZnO PhCS, we fabricated patterns of different lattice constant a from 110nm to 130nm with finer steps with $r/a = 0.25$. All the patterns are $8\mu m \times 8\mu m$ and without intentionally introduced structure defect, the ensemble averaged lasing threshold exhibit a pronounce minimum at $a = 115 - 130nm$ as shown in Fig. 5(a). While the lasing wavelength for different pattern is plotted in Fig. 5(b). One can see that the lasing wavelength is almost linearly scaled with lattice constant a, which is also a direct proof that the lasing modes are related to the in plane photonic band gaps. The two dash lines describe the edge of gain spectrum of ZnO, thus the dip in the measured threshold in Fig. 5(a) is attributed to spectral overlap of the lasing frequencies with ZnO gain spectrum. We also take the near field images of the lasing modes in all the patterns. Interestingly, some of the modes are spatially localized, while some are spatially extended. Fig. 6 shows one typical lasing mode with extended spatial profile. The fact that we can get both localized and extended modes make us believe that all the modes are defect modes from the photonic structures. Because the band gap is very narrow, the unavoidable defects introduced during fabrication make such gap shallower and even narrower. For some pattern, some extended mode close to dielectric band edge of the gap has highest quality factor and lases first, while for other pattern, some localized mode close to the center of the gap has highest quality factor and lases first. Which kind of modes has higher quality factor really depends on the particular

fabrication defects configuration in the pattern.

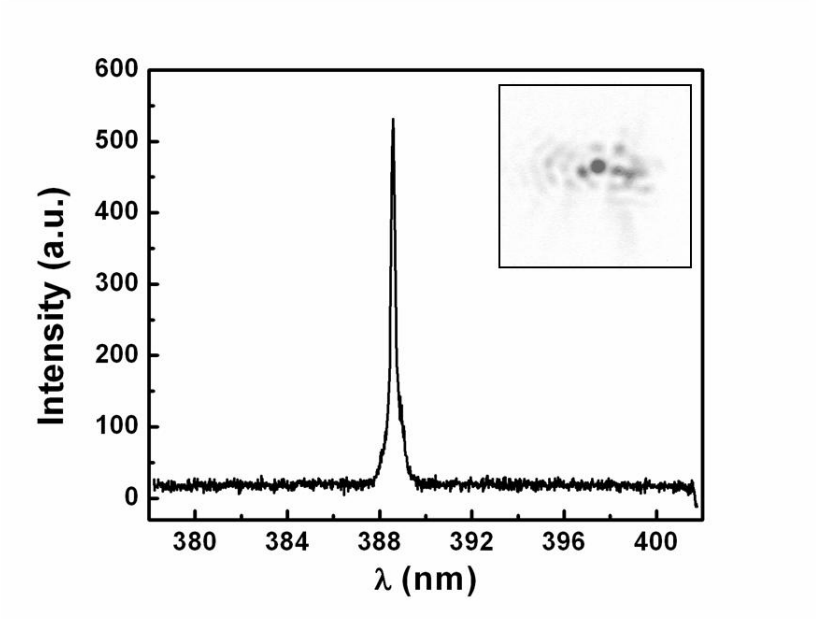

Figure 6. A typical lasing spectrum for a extended defect mode close to dielectric band edge. Pump pulse energy: 2.0nJ. Inset: near field image of the lasing mode, the square boundary represents the boundary of the PhCS pattern.

4. DISCUSSION AND CONCLUSION

For a PhCS laser cavity, light may escape vertically through the top/bottom interfaces into air/substrate or laterally via the edge of the periodic pattern into air or unpatterned part of the slab. The vertical leakage rate is characterized by the out-of-plane energy loss per optical cycle $Q_{\perp}^{-1}$, and the lateral by $Q_{//}^{-1}$. A defect state spatially localized in plane has a large distribution of $k_{//}$, thus typically has large leakage in the vertical direction, i.e., $Q_{\perp}^{-1} >> Q_{//}^{-1}$. For a extended bandedge state, the $k_{//}$ distribution is small, so the lateral leakage usually dominates over the vertical one, $Q_{//}^{-1} >> Q_{\perp}^{-1}$. The total loss is described by $Q_{tot}^{-1} = Q_{\perp}^{-1} + Q_{//}^{-1}$. Low lasing threshold demands maximization of Q_{tot}, which is hindered by $Q_{\perp}$ for a localized defect state and $Q_{//}$ for a extended bandedge state. To improve Q_{tot}, many works have been done to increase $Q_{\perp}$ for a localized defect cavity state.

We realize that in the case of either intentionally introduced localized defect state or extended bandedge in a perfect periodic structure without defects, one of the Q component is much larger than the other, and the Q_{tot} is determined mainly by the smaller one. when certain degree of defects are introduced into the PhCS structure, we find that the two Q components are balanced to certain extent, which will increase Q_{tot}.[20] In particular, for a localized defect state, introducing defects around the original defect cavity will reduce $Q_{//}$, thus the spatial extent in plane is increased, in return, the leakage in vertical direction is reduced since the $k_{//}$ distribution is decreased. Because in this case $Q_{\perp}^{-1} >> Q_{//}^{-1}$ and Q_{tot} is dominated by $Q_{\perp}$, when we increase $Q_{\perp}$, Q_{tot} is increased though $Q_{//}$ is reduced. Similar principle can be applied to extended bandedge state. By introducing certain defect, the mode spatial extent can be reduced and thus $Q_{//}$ is increased, while $Q_{\perp}$ is reduced, but Q_{tot} is increased over all. In our ZnO PhCS, due to the small feature size of periodic structure in plane, certain structure defects are unavoidable during FIB fabrication, e.g., the deviation of shape of air cylinder from perfect

circle, the shape and average radius difference for different air cylinders, the deviation of air cylinder center position from perfect triangular lattice. These defects can help to balance different Q component and optimize Q_{tot}. It explains the surprising experimental result that even with such narrow in plane photonic band gap and certain structure defects presented, lasing can still achieved from this ZnO PhCS samples. We would like to point out that all the defects are not intentionally introduced in our ZnO PhCS patterns, which really relieve the technical challenge of structure fine tuning in intentionally designed defect cavity fabrication. While this is an experimental advantage, fine control of the structure is lost and we have to live with the patterns we get. This means that the performance of our PhCS laser can be further improved by carefully pattern design and fabrication with higher precision. Another potential fact to hinder our ZnO PhCS laser performance is the optical quality damage by the FIB etching technique. Even we recovered the photoluminescence partially by post thermal annealing, a better etching technique without structure damage or better means to recover the crystalline quality wound lower the PhCS laser threshold even further.

In conclusion, we designed and fabricated ZnO PhCS structure with FIB etching technique, and lasing in UV region at room temperature has been achieved under optical pumping. By change the lattice constant, fine tuning of lasing wavelength has been realized for a 20nm range. Though certain structure defects are unavoidable from sample fabrication, such defects are thought to help to optimize the lasing performance. With better pattern design and fabrication precision, as well as material quality improvement, lower lasing threshold would be expected.

ACKNOWLEDGMENTS

This work was supported by the National Science Foundation under the Grant no. ECS-0244457.

REFERENCES

1. C. M. Soukoulis, ed. "*Photonic Crystals and Light Localization in the 21st Century*" (Kluwer Academic, Dordrecht, 2001).
2. J. Vučkovič, M. Lončar, H. Mabuchi, and A, Scherer, *Design of photonic crystal microcavities for cavity QED* Phys. Rev. E **65**, 016608 (2001).
3. K. Srinivasan, and O. Painter, *Momentum space design of high-Q photonic crystal optical cavities* Opt. Express **10**, 670 (2002).
4. Y. Akahane, T. Asano, B. Song, and S. Noda, *High-Q photonic nanocavity in a two-dimensional photonic crystal* Nature **425**, 944 (2003).
5. B. Song, S. Noda, T. Asano, and Y. Akahane, *Ultra-high-Q photonic double-heterostructure nanocavity* Nature Materials, **4**, 207 (2005).
6. D. Englund, I. Fushman, and J. Vučkovič, *General recipe for designing photonic crystal cavities* J. Opt. Express **13**, 5961 (2005).
7. O. Painter, R. K. Lee, A. Scherer, A. Yariv, J. D. O'Brien, P. D. Dapkus, and I. Kim, *Two-dimensional photonic band-gap defect mode laser* Science **284**, 1819 (1999).
8. M. Imada, S. Noda, A. Chutinan, T. Tokuda, M. Murata, and G. Sasaki, *Coherent two-dimensional lasing action in surface-emitting laser with triangular-lattice photonic crystal structure* Appl. Phys. Lett. **75**, 316 (1999).
9. H. Ryu, S. Kwon, Y. Lee, Y. Lee, and J. Kim *Very-low-threshold photonic band-edge lasers from free-standing triangular photonic crystal slabs* Appl. Phys. Lett. **80** 3476 (2002).
10. H. Park, S. Kim, S. Kwon, Y. Ju, J. Yang, J. Baek, S. Kim, and Y. Lee *Electrically Driven Single-Cell Photonic Crystal Laser* Science **305** 1444 (2004).
11. J. Shakya, K. H. Kim, J. Y. Lin, and H. X. Jiang, *Enhanced light extraction in III-nitride ultraviolet photonic crystal light-emitting diodes* Appl. Phys. Lett. **85**, 142 (2004).
12. X. Wu, A. Yamilov, X. Liu, S. Li, V. P. Dravid, R. P. H. Chang, and H. Cao, *Ultraviolet photonic crystal laser* Appl. Phys. Lett. **85**, 3657 (2004).

13. S. G. Johnson, and J. D. Joannopoulos, *Block-iterative frequency-domain methods for Maxwell's equations in a planewave basis* Opt. Exp. **8**, 173 (2001).
14. A. Yamilov and H. Cao, *Highest-quality modes in disordered photonic crystals* Phys. Rev. A **69**, 031803 (2004).
15. A. Yamilov, X. Wu, and H. Cao, *Photonic band structure of ZnO photonic crystal slab laser* J. Appl. Phys. **98** 103102 (2005).
16. S. G. Johnson, S. Fan, P. R. Villeneuve, J. D. Joannopoulos, and L. A. Kolodziejski, *Guided modes in photonic crystal slabs* Phys. Rev. B **60**, 5751 (1999).
17. E. Chow, S. Lin, S. G. Johnson, P. R. Villeneuve, J. D. Joannopoulos, J. R. Wendt, G. A. Vawter, W. Zubrzycki, H. Hou, and A. Alleman, *Three-dimensional control of light in a two-dimensional photonic crystal slab* Nature **407**, 983 (2000).
18. Y. S. Park, C. W. Litton, T. C. Collins, and D. C. Reynolds, *Exciton spectrum of ZnO* Phys. Rev. **143** 143 (1966).
19. S. Jung, W. Park, H. Cheong, G. Yi, H. Jang, S. Hong, and T. Joo, *Time-resolved and time-integrated photoluminescence in ZnO epilayers grown on Al_2O_3(0001) by metalorganic vapor phase epitaxy* Appl. Phys. Lett. **80** 1924 (2002).
20. A. Yamilov, X. Wu, X. Liu, R. P. H. Chang, and H. Cao, *Self-optimization of optical confinement in ultraviolet photonic crystal slab laser* in process.